

## Effect of Low Magnetic Field on Dose Distribution in the Partial-Breast Irradiation

Jung-in Kim<sup>\*†‡§</sup>, So-Yeon Park<sup>\*†‡||</sup>, Yang Hoon Lee<sup>\*</sup>, Kyung Hwan Shin<sup>\*†‡||</sup>,  
Hong-Gyun Wu<sup>\*†‡||</sup>, Jong Min Park<sup>\*†‡§</sup>

<sup>\*</sup>Department of Radiation Oncology, Seoul National University Hospital, Seoul,

<sup>†</sup>Biomedical Research Institute, Seoul National University Hospital, Seoul,

<sup>‡</sup>Institute of Radiation Medicine, Seoul National University Medical Research Center, Seoul,

<sup>§</sup>Center for Convergence Research on Robotics, Advanced Institutes of Convergence Technology, Suwon,

<sup>||</sup>Interdisciplinary Program in Radiation Applied Life Science, Seoul National University College of Medicine, Seoul,

<sup>¶</sup>Department of Radiation Oncology, Seoul National University College of Medicine, Seoul, Korea

The aim of this study is to investigate the effect of low magnetic field on dose distribution in the partial-breast irradiation (PBI). Eleven patients with an invasive early-stage breast carcinoma were treated prospectively with PBI using 38.5 Gy delivered in 10 fractions using the ViewRay<sup>®</sup> system. For each of the treatment plans, dose distribution was calculated with magnetic field and without magnetic field, and the difference between dose and volume for each organ were evaluated. For planning target volume (PTV), the analysis included the point minimum ( $D_{min}$ ), maximum, mean dose ( $D_{mean}$ ) and volume receiving at least 90% ( $V_{90\%}$ ), 95% ( $V_{95\%}$ ) and 107% ( $V_{107\%}$ ) of the prescribed dose, respectively. For organs at risk (OARs), the ipsilateral lung was analyzed with  $D_{mean}$  and the volume receiving 20 Gy ( $V_{20\text{ Gy}}$ ), and the contralateral lung was analyzed with only  $D_{mean}$ . The heart was analyzed with  $D_{mean}$ ,  $D_{max}$ , and  $V_{20\text{ Gy}}$ , and both inner and outer shells were analyzed with the point  $D_{min}$ ,  $D_{max}$  and  $D_{mean}$ , respectively. For PTV, the effect of low magnetic field on dose distribution showed a difference of up to 2% for volume change and 4 Gy for dose. In OARs analysis, the significant effect of the magnetic field was not observed. Despite small deviation values, the average difference of mean dose values showed significant difference ( $p < 0.001$ ), but there was no difference of point minimum dose values in both shell structures. The largest deviation for the average difference of  $D_{max}$  in the outer shell structure was  $5.0 \pm 10.5$  Gy ( $p = 0.148$ ). The effect of low magnetic field of 0.35 T on dose deposition by a Co-60 beam was not significantly observed within the body for PBI IMRT plans. The dose deposition was only appreciable outside the body, where a dose build-up due to contaminated electrons generated in the treatment head and scattered electrons formed near the body surface.

**Key Words:** Low magnetic field, Dose distribution, Partial breast irradiation, MRI-guided radiation therapy system, IMRT

### Introduction

Partial breast irradiation (PBI) is a radiation treatment for selected patients with early-stage breast cancer which the portion of the breast at the highest risk of recurrence (the lumpectomy cavity plus a limited amount of surrounding tissues).<sup>1,2)</sup> Several distinct treatment techniques have been used to deliver this therapy, including multicatheter interstitial brachytherapy, single-entry intracavitary brachytherapy catheters, intraoperative techniques (x-rays and electrons), and external radiation with photons and/or protons.<sup>3-7)</sup> Each modality has been reported ad-

This research was supported by a grant of the Korea Health Technology R&D Project through the Korea Health Industry Development Institute (KHIDI), funded by the Ministry of Health & Welfare, Republic of Korea (grant number: HI14C3459).

Received 8 December 2015, Revised 17 December 2015, Accepted 18 December 2015

**Correspondence:** Jong Min Park (leodavinci@naver.com)

Tel: 82-2-2072-2527, Fax: 82-2-765-3317

© This is an Open-Access article distributed under the terms of the Creative Commons Attribution Non-Commercial License (<http://creativecommons.org/licenses/by-nc/4.0>) which permits unrestricted non-commercial use, distribution, and reproduction in any medium, provided the original work is properly cited.

advantages and disadvantages, depending on the patient's anatomy and preference, as well as the resources available at a particular radiation oncology facility.<sup>5,8,9)</sup> External beam radiation therapy (EBRT), which can be delivered noninvasively, is most common type to deliver PBI using the standard linear accelerator (linac) found in all radiation oncology facilities. Many studies have shown the long- and short-term effectiveness of EBRT.<sup>10,11)</sup> Recently, a commercial MR-IGRT system (ViewRay<sup>®</sup>, ViewRay Inc., Cleveland, OH, USA) has been implemented in the clinic as a EBRT machine. The ViewRay<sup>®</sup> system consists of an on-board MR imaging system with 0.35 T low magnetic field and a radiation therapy system with tri Co-60 sources.<sup>12)</sup> The application of the magnetic field to a volume undergoing irradiation by a photon beam can produce localized regions of dose enhancement and dose reduction. The consequences of these changes on dose distribution for radiotherapy treatment with a magnetic field have been studied by many groups using analytical, simulation and/or experimental techniques.<sup>13-15)</sup> Largely, the focus has been on changes to the spatial distribution of dose resulting from the magnetic field influence on charged particle transport. The high magnetic field strength can have significant perturbations on dose distributions, such as changes to the percentage depth dose, tissue interface effects and lateral shifts in dose distributions in the photon beam radiotherapy.<sup>15-17)</sup> The aim of this work was to investigate the consequences to radiation dose distributions that occur in low magnetic field strengths of 0.35 T in comparison with the zero magnetic field in PBI intensity modulated radiation therapy (IMRT) plans.

## Materials and Methods

### 1. Patient selection and treatment planning setup

Eleven patients with invasive early-stage breast carcinoma have been treated at Seoul National University Hospital (SNUH) with PBI using the ViewRay<sup>®</sup> system from October, 2015. All eligible patients had Stage I~II breast cancer and were treated with static IMRT techniques using 38.5 Gy delivered in 10 fractions. The planning target volume (PTV) consists of the gross tumor volume (GTV) corresponding to the lumpectomy cavity plus a 1.0~2.0 cm margin. The size of the PTV is  $99.5 \pm 41.5 \text{ cm}^3$  ( $41.5 \sim 204.99 \text{ cm}^3$ ). Several organs at

risk (OAR) were contoured: heart, contralateral and ipsilateral lungs. Especially, two shell structures were generated to investigate the effect of low magnetic field on dose distribution near the body outline of the patients. One was the inner shell of 0.3 cm thickness inside the body surface. The other was the outer shell of 0.3 cm thickness outside the body surface. The ViewRay<sup>®</sup> system has a total of three Co-60 sources, dose rate is 550 cGy/min, spaced a fixed 120° apart. The 60 multi-leaf collimators (MLCs) (two opposing banks of 30), a double-focused MLC to minimize the penumbra, are 1.05 cm wide at isocenter of 105 cm (covering a square field of  $27.3 \times 27.3 \text{ cm}^2$ ). The ViewRay<sup>®</sup> treatment planning system was used to make IMRT plans for PBI. A plan was created with 3~7 groups for a total of 6~15 multiple directional beams depending on the target location and size. The ViewRay<sup>®</sup> treatment planning system provides its own novel optimization algorithm and a full Monte Carlo (MC)-based algorithm for dose calculation. In this study, the IMRT efficiency, which optimizes a relatively smoother fluence map, was set at the value of 1.0. The IMRT level, which discretizes each fluence map into deliverable beam-on segments, was set at the value of 3.0. The resolution of dose grid was set at the default value of 0.3 cm. Each of the treatment plans were applied with both options for dose calculation with magnetic field and without magnetic field MC algorithms.

### 2. Dose volume analysis

The effect of low magnetic field on dose distribution was investigated through dose volume histogram (DVH). For PTV, the analysis included the point minimum ( $D_{\min}$ ), maximum, mean dose ( $D_{\text{mean}}$ ) and volume receiving at least 90% ( $V_{90\%}$ ), 95% ( $V_{95\%}$ ) and 107% ( $V_{107\%}$ ) of the prescribed dose, respectively. For OARs, the ipsilateral lung was analyzed with  $D_{\text{mean}}$  and the volume receiving 20 Gy ( $V_{20 \text{ Gy}}$ ), and the contralateral lung was analyzed with only  $D_{\text{mean}}$ . The heart was analyzed with  $D_{\text{mean}}$ ,  $D_{\text{max}}$ , and  $V_{20 \text{ Gy}}$ , and both inner and outer shells were analyzed with the point  $D_{\min}$ ,  $D_{\text{max}}$ , and  $D_{\text{mean}}$ , respectively. Average DVHs were analyzed from the DVHs of each patient to obtain average values at each dose and volume levels. The difference of dose or volume in the DVH analysis was calculated as follows.

Difference=the value with magnetic field—the value without magnetic field

T-test with 95% confidence was used to assess the statistical significance of the difference between the values with magnetic field and without magnetic field.

## Results

The comparison of dose distributions for the case of PBI patient with magnetic field and without magnetic field was shown in Fig. 1. The magnetic field was applied when the dose distribution was calculated with the magnetic field. To investigate differences in the relative dose distribution, results of the dose volume analysis were described for different structures.

### 1. Dose distribution change in PTV

The PTV dose calculations were compared with low magnetic field and zero magnetic field. The average difference of mean dose values was  $0.1 \pm 0.1$  Gy ( $p=0.003$ ). For the point dose analysis, the average differences of  $D_{min}$  and  $D_{max}$  were

$1.7 \pm 1.8$  Gy ( $p=0.011$ ) and  $1.0 \pm 0.3$  Gy ( $p=0.351$ ), respectively. The average difference of volumes,  $V_{90\%}$ ,  $V_{95\%}$ , and  $V_{107\%}$ , was less than 1%. The positive value of the difference means that the dose in PTV increases with low magnetic field compared to zero magnetic field. However, these results showed the average difference value. Fig. 2 describes the difference for each patient in the PTV dose volume analysis. Comparison of the PTV structure for low magnetic field with respect to the zero magnetic field showed maximum deviations in the order of 2% and 4 Gy. Table 1 demonstrates the analysis of the average dose volume difference for PTV.

### 2. Dose distribution change in OARs

Table 2 demonstrates the analysis of the average dose volume difference for ipsilateral lung, contralateral lung, and heart. There was no average difference of  $D_{mean}$  in ipsilateral lung and  $V_{20\text{ Gy}}$  in heart. The average difference of the volume  $V_{20\text{ Gy}}$  was  $-0.1 \pm 0.2$  Gy ( $p=0.116$ ) in ipsilateral lung, and  $-0.1 \pm 0.4$  Gy ( $p=0.312$ ) in contralateral lung. In the heart analysis, the average differences of  $D_{mean}$  and  $D_{max}$  are  $0.1 \pm 0.3$  Gy ( $p=0.359$ ) and  $0.4 \pm 1.8$  Gy ( $p=0.484$ ), respectively. In these OARs analysis, the significant difference was not observed.

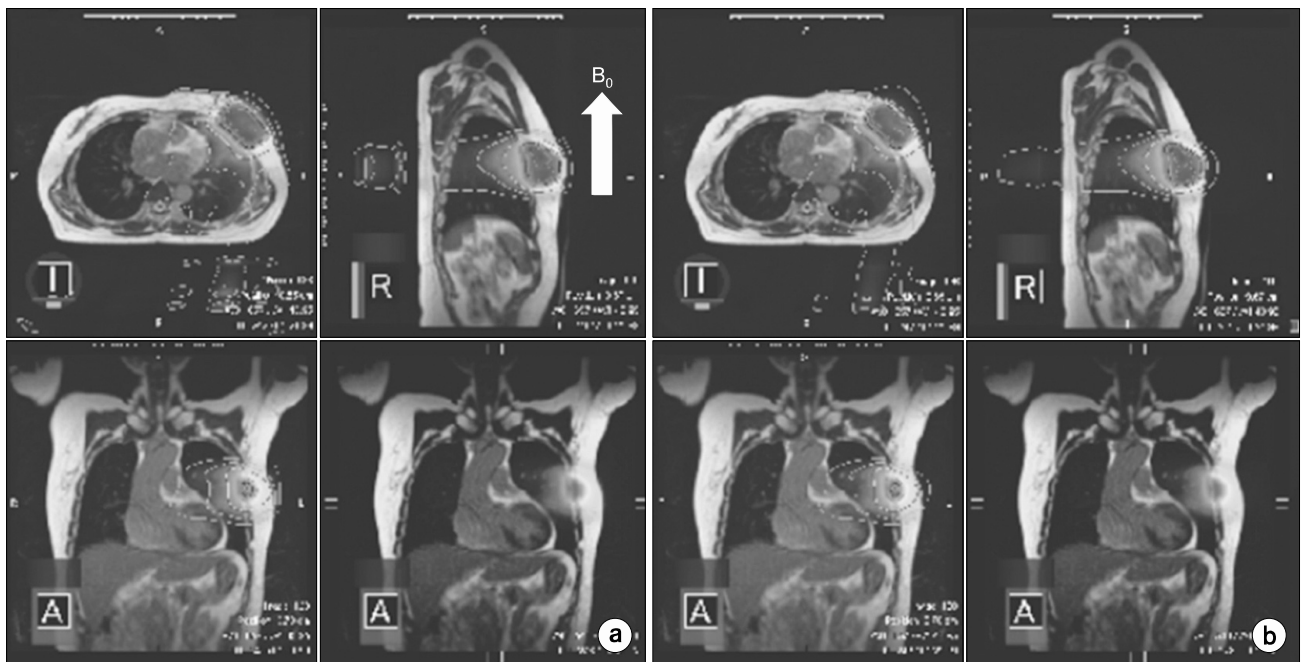


**Fig. 1.** The comparison of dose distribution for (a) with magnet field and (b) without magnet field in the case of PBI patient with a magnet field ( $B_0$ ).

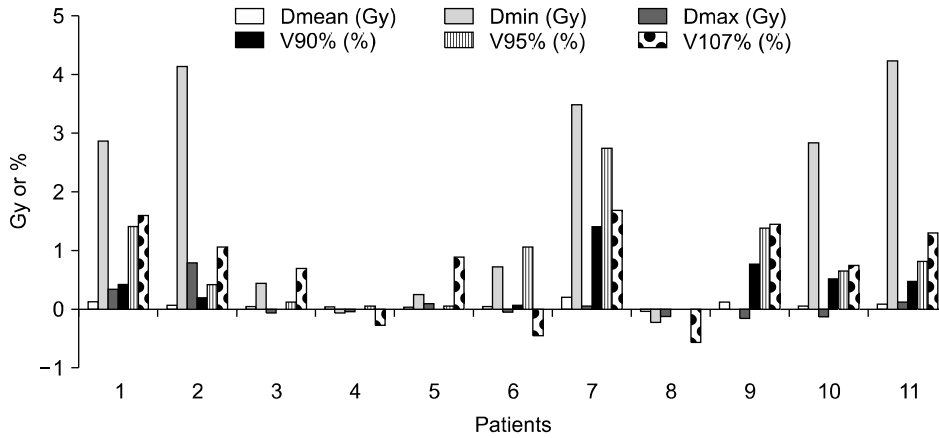


**Fig. 2.** Dose and Volume difference values in PTV for each patients.

**Table 1.** The average dose volume analysis for PTV.

Analysis	With Magnet	Without Magnet	Difference value	p-value
$D_{\text{mean}}$ (Gy)	$40.7 \pm 0.4$	$40.6 \pm 0.4$	$0.1 \pm 0.1$	0.003
$D_{\text{min}}$ (Gy)	$30.4 \pm 10.0$	$28.7 \pm 9.6$	$1.7 \pm 1.8$	0.011
$D_{\text{max}}$ (Gy)	$44.0 \pm 0.5$	$43.9 \pm 0.4$	$1.0 \pm 0.3$	0.351
$V_{90\%}$ (%)	$99.9 \pm 0.1$	$99.5 \pm 0.5$	$0.4 \pm 0.4$	0.025
$V_{95\%}$ (%)	$98.9 \pm 0.6$	$98.1 \pm 1.2$	$0.8 \pm 0.8$	0.01
$V_{107\%}$ (%)	$39.7 \pm 10.7$	$39.0 \pm 10.9$	$0.7 \pm 0.8$	0.013

**Table 2.** The average dose volume analysis for organs at risk (OARs).

OAR	Analysis	With Magnet	Without Magnet	Difference value	p-value
Ipsilateral lung	$D_{\text{mean}}$ (Gy)	$7.7 \pm 1.8$	$7.7 \pm 1.8$	$0.0 \pm 0.04$	1.000
	$V_{20 \text{ Gy}}$ (%)	$6.8 \pm 4.2$	$6.9 \pm 4.3$	$-0.1 \pm 0.2$	0.116
Contralateral lung	$D_{\text{mean}}$ (Gy)	$2.1 \pm 1.0$	$2.2 \pm 1.0$	$-0.1 \pm 0.4$	0.312
Heart	$D_{\text{mean}}$ (Gy)	$4.7 \pm 3.8$	$4.6 \pm 3.8$	$0.1 \pm 0.3$	0.359
	$D_{\text{max}}$ (Gy)	$23.5 \pm 11.1$	$23.1 \pm 11.8$	$0.4 \pm 1.8$	0.484
	$V_{20 \text{ Gy}}$ (%)	$2.1 \pm 3.7$	$2.1 \pm 3.7$	$0.0 \pm 0.01$	0.221

### 3. Dose distribution change near the body surface

Table 3 demonstrates the analysis of the average dose difference for shell structures. Despite small deviation values, the average difference of mean dose values showed significant difference ( $p < 0.001$ ), but there was no difference of point minimum dose values in both shell structures. The average difference of  $D_{\text{max}}$  was  $0.2 \pm 0.4$  Gy ( $p = 0.143$ ) in the inner shell structure. However, the largest deviation for the average difference of  $D_{\text{max}}$  in the outer shell structure was  $5.0 \pm 10.5$  Gy ( $p = 0.148$ ). Fig. 3 describes the dose distribution in sagittal images between with the magnetic field and without magnetic

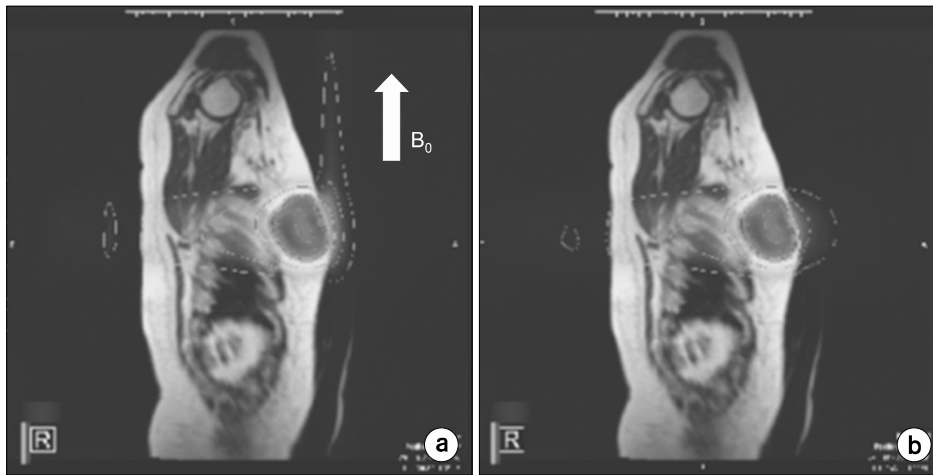
field. A longitudinal magnetic field shows dose deposition outside the body since the secondary electrons scattered from the body and generated in the treatment head travel in the direction of the magnetic field.

### Discussion

The ViewRay<sup>®</sup> treatment planning system uses two methods of MC dose computation algorithms of with magnetic field and without magnetic field. Both MC algorithms adopt the same techniques to perform a highly optimized simulation of the photons using a variety of variance reduction techniques.<sup>[12]</sup>

**Table 3.** The average dose analysis for shell structures.

Structure	Analysis	With magnet	Without magnet	Difference value	p-value
Inner shell	$D_{\text{mean}}$ (Gy)	$1.53 \pm 0.5$	$1.49 \pm 0.5$	$0.04 \pm 0.01$	$< 0.001$
	$D_{\text{min}}$ (Gy)	$0.0 \pm 0.0$	$0.0 \pm 0.0$	$0.0 \pm 0.01$	0.176
	$D_{\text{max}}$ (Gy)	$42.5 \pm 1.8$	$42.3 \pm 1.6$	$0.2 \pm 0.4$	0.143
Outer shell	$D_{\text{mean}}$ (Gy)	$1.17 \pm 0.4$	$1.04 \pm 0.4$	$0.13 \pm 0.1$	$< 0.001$
	$D_{\text{min}}$ (Gy)	$0.0 \pm 0.0$	$0.0 \pm 0.0$	$0.0 \pm 0.01$	0.221
	$D_{\text{max}}$ (Gy)	$37.5 \pm 13.1$	$32.5 \pm 6.6$	$5.0 \pm 10.5$	0.148

**Fig. 3.** The dose distribution in sagittal image between (a) with magnet field ( $B_0$ ) and (b) without magnet field.

The MC algorithm without magnetic field tracks only the photons through the patient geometry without considering the magnetic field. However, the MC with the magnetic field includes the effect of the magnetic field when tracking charged particles. When a photon beam irradiates without a magnetic field, charged particles travel into media and produces a large number of electrons in a predominantly forward direction. These electrons deposit dose along their path.<sup>18,19)</sup> However, the secondary electrons in the presence of the magnetic field are deflected by the Lorentz force. The electrons travel in a series of arc-shaped trajectories, no longer a helical trajectory, in tissue or water. If the scattering electrons enter into the low-density media like air, their helical trajectories can be fulfilled again and these electrons return into tissue with longer mean free path. This phenomenon is called the electron return effect (ERE).<sup>20)</sup> The return of secondary electrons into the tissue causes dose increase at all tissue-air boundaries. Esmaeeli et al. studied the effect of the uniform high magnetic field on dose distribution in the breast radiotherapy and concluded that the magnetic field can reduce significantly the dose to the in-

ternal and contralateral tissues and increase it to the PTV.<sup>21)</sup> In our study, the effect of the magnetic field on dose distribution was not significantly observed in internal tissues and in PTV. Outside the body, however, there was a noticeable dose increase along to the magnetic field direction. Esmaeeli et al. used the high magnet field of 1.5 T and 3.0 T, and a 6 MV opposed parallel beams described as being tangential to the chest wall. These parallel beam easily caused ERE, which reduced dose in lung as low-density media close to chest wall as the dense one. In our study, with low magnetic field of 0.35 T, the multiple direction of photon beams was used for IMRT plans decentered the secondary electrons deflected by the Lorentz force. Furthermore, in the ViewRay<sup>®</sup> treatment planning system, the default history setting will achieve about 1% statistical uncertainty for a dose grid of 0.3 cm. The differences for dose and volume analysis within the body were included on this statistical uncertainty. There was no considerable difference ( $p > 0.05$ ) between with magnetic field and without magnetic field excluding  $D_{\text{mean}}$  and  $D_{\text{min}}$  in PTV and  $D_{\text{mean}}$  in both shell structures. The scope of this study was lim-

ited in the single treatment site of PBI and relatively a small sample size. Further studies are necessary in order to confirm the effect of low magnetic field on dose distribution based on various treatment sites and measurements with large sample sizes.

### Conclusion

The effect of the magnetic field strength of 0.35 T on dose deposition by a Co-60 beam was not significantly observed within the body for PBI IMRT plans. The dose deposition was only appreciable outside the body, where a dose build-up due to contaminated electrons generated in the treatment head and scattered electrons formed near the body surface.

### References

1. Beitsch PD, Shaitelman SF, Vicini FA: Accelerated partial breast irradiation. *J Surg Oncol.* 103(4):362–368 (2011).
2. Alvarez C: Accelerated partial breast irradiation. *J Am Coll Surg.* 209(6):795–796 (2009).
3. McIntosh A, Read PW, Khandelwal SR, et al.: Evaluation of coplanar partial left breast irradiation using tomotherapy-based topotherapy. *Int J Radiat Oncol Biol Phys.* 71(2): 603–610 (2008).
4. Kozak KR, Smith BL, Adams J, et al.: Accelerated partial-breast irradiation using proton beams: initial clinical experience. *Int J Radiat Oncol Biol Phys.* 66(3):691–698 (2006).
5. Wilder RB, Curcio LD, Khanijou RK, et al.: A Contura catheter offers dosimetric advantages over a MammoSite catheter that increase the applicability of accelerated partial breast irradiation. *Brachytherapy.* 8(4):373–378 (2009).
6. Weed DW, Edmundson GK, Vicini FA, et al.: Accelerated partial breast irradiation: a dosimetric comparison of three different techniques. *Brachytherapy.* 4(2):121–129 (2005).
7. Stewart AJ, Khan AJ, Devlin PM: Partial breast irradiation: a review of techniques and indications. *Br J Radiol.* 83(989): 369–378 (2010).
8. Mydin AR, Gaffney H, Bergman A, et al.: Does a three-field electron/mini-tangent photon technique offer dosimetric advantages to a multifield, photon-only technique for accelerated partial breast irradiation?. *Am J Clin Oncol.* 33(4):336–340 (2010).
9. Bourcier C, Taghian A, Marsiglia H: Three-field electron/mini-tangent photon technique offer dosimetric advantages to a multifield, photon-only technique for accelerated partial breast irradiation if well implemented. *Am J Clin Oncol.* 34(6):648 (2011).
10. Vera R, Trombetta M, Mukhopadhyay ND, et al.: Long-term cosmesis and toxicity following 3-dimensional conformal radiation therapy in the delivery of accelerated partial breast irradiation. *Pract Radiat Oncol.* 4(3):147–152 (2014).
11. Galland-Girodet S, Pashtan I, MacDonald SM, et al.: Long-term cosmetic outcomes and toxicities of proton beam therapy compared with photon-based 3-dimensional conformal accelerated partial-breast irradiation: a phase 1 trial. *Int J Radiat Oncol Biol Phys.* 90(3):493–500 (2014).
12. Mutic S, Dempsey JF: The ViewRay system: magnetic resonance-guided and controlled radiotherapy. *Semin Radiat Oncol.* 24(3):196–199 (2014).
13. Rubinstein AE, Liao Z, Melancon AD, et al.: Technical Note: A Monte Carlo study of magnetic-field-induced radiation dose effects in mice. *Med Phys.* 42(9):5510–5516 (2015).
14. Burke B, Ghila A, Fallone BG, et al.: Radiation induced current in the RF coils of integrated linac-MR systems: the effect of buildup and magnetic field. *Med Phys.* 39(8):5004–5014 (2012).
15. Kirkby C, Stanescu T, Fallone BG: Magnetic field effects on the energy deposition spectra of MV photon radiation. *Phys Med Biol.* 54(2):243–257 (2009).
16. Wen Z, Pelc NJ, Nelson WR, et al.: Study of increased radiation when an x-ray tube is placed in a strong magnetic field. *Med Phys.* 34(2):408–418 (2007).
17. Shen CS: adiation problems in a strong magnetic field. *Ann N Y Acad Sci.* 257:44–55 (1975).
18. Al-Basheer AK, Sjoden GE, Ghita M: Electron Dose Kernels to Account for Secondary article Transport in Deterministic Simulations. *Nucl Technol.* 168(3):906–918 (2009).
19. Kim JO, Kim JK: ose equivalent per unit fluence near the surface of the ICRU phantom by including the secondary electron transport for photons. *Radiat Prot Dosimetry.* 83(3):211–219 (1999).
20. Raaijmakers AJE, Raaymakers BW, Lagendijk JJW: Integrating a MRI scanner with a 6 MV radiotherapy accelerator: dose increase at tissue-air interfaces in a lateral magnetic field due to returning electrons. *Phys Med Biol.* 50(7):1363–1376 (2005).
21. Esmaeeli AD, Pouladian M, Monfared AS, et al.: Effect of uniform magnetic field on dose distribution in the breast radiotherapy. *Int J Radiat Res.* 12(2):151–160 (2014).

## 부분유방 방사선조사 시 저자기장이 선량분포에 미치는 영향

\*서울대학교병원 방사선종양학과, <sup>†</sup>서울대학교병원 의생명연구원, <sup>‡</sup>서울대학교 의학연구원 방사선의학연구소,  
<sup>§</sup>차세대융합기술연구원 로봇융합연구센터, <sup>||</sup>서울대학교 의과대학 방사선응용생명과학 협동과정,  
<sup>¶</sup>서울대학교 의과대학 방사선종양학교실

김정인\*<sup>†‡§</sup> · 박소연\*<sup>†‡||</sup> · 이양훈\* · 신경환\*<sup>†‡¶</sup> · 우홍균\*<sup>†‡¶</sup> · 박종민\*<sup>†‡§</sup>

이 연구 목적은 부분유방 방사선조사 시 저자기장이 선량분포에 주는 영향을 조사하는 것이다. 11명의 초기 유방암 환자들이 브레이 시스템에서 38.5 Gy를 10회의 부분유방 방사선 조사 방법으로 치료를 받았다. 모든 치료계획은 저자기장이 있을 때와 없을 때의 선량분포를 각각 계산하고, 각 구조물에 대하여 선량과 용적의 차이값을 평가하였다. 치료계획용적에 대해서는 평균선량, 최소, 최대 선량 그리고 처방선량의 최소한 90%, 95%, 107%를 조사받는 용적을 각각 분석에 포함하였다. 정상조직장기 중 치료와 동일한 방향 폐는 평균선량, 20 Gy를 받는 용적을 평가하고, 반대방향의 폐는 평균선량만 평가하였다. 심장은 평균선량, 최대선량과 20 Gy를 받는 용적을 각각 평가하였다. 내 · 외각 껍질구조에 대해서는 평균선량, 최소, 최대 선량을 각각 평가하였다. 치료계획용적의 경우 저자기장에 의한 선량 분포의 영향은 최대 2%의 용적 변화, 4 Gy 선량 변화 차이를 보였다. 정상조직 장기에 대해서는 자기장에 의한 선량 분포의 영향은 발견되지 않았다. 내 · 외각 껍질구조에서 두 선량분포 계산에서 평균값의 차이는 작지만 평균선량의 차이가 유효하게 나타났다. 최소 선량 분석에서는 내 · 외각 껍질구조에서 차이가 없었다. 자기장에 의한 선량 분포의 영향은 외각 껍질구조에서 최대선량 값 분석에서  $5.0 \pm 10.5$  Gy로 나타났다. Co-60 빔을 이용한 세기조절 방사선치료계획의 부분유방 방사선조사 치료에서 0.35 T 저자기장에 의한 선량 분포 영향은 인체 내부에서는 크게 발견되지 않았다. 다만 인체 외부에서 선량 증가가 관찰되었고, 이는 치료시스템 헤드에서 발생하는 이차전자와 인체 표면 부근에서 산란된 이차전자가 자기장의 방향으로 이동하면서 선량 분포를 형성하고 있다.

**중심단어:** 저자기장, 선량 분포, 부분유방 방사선조사, 자기공명영상기반 방사선치료, 세기조절방사선치료